IMPURITY DISTRIBUTION IN SUBMERGED HEATING METHOD WITH AND WITHOUT ROTATION

Alexsey I. Fedyushkin and Nicolai.G. Bourago

The Institute for Problems in Mechanics, Russian Academy of Sciences,
Prospect Vernadskogo 101, Moscow, 117526, Russia.
Tel.:+7-095-4343283, fax: +7-095-9382048, e-mail: fai@ipmnet.ru

ABSTRACT

Results of unsteady 2D Navier-Stokes mathematical modeling of convection-diffusion processes are presented. The equations are solved by finite element method in the cylindrical region. Taking into account a calculated history of dopant concentration at the surface of the crystallization we determine a distribution of the dopant concentration in crystal .An influence of steady and oscillatory rotation of submerged heater on distribution of dopant in crystals is investigated.

INTRODUCTION

Dependence and strong sensitivity of dopant concentration in semiconductor melts on various conditions of growth such as geometry, heat and dynamic effects, convection (gravity and forced), rotation, vibration etc., are known and published in many papers (see for instance (see reference, for example, Polezhaev (1994), Nikitin et al. (1981), Zharikov et al. (1990), Meyer et al. (1997), Golyshev et al (1995), Ostrogorsky et al. (1995, 1998), Bourago et al. (1997, 1998)). The goal of such investigations is to find out how to govern these processes and dopant concentration. A classification of methods of governing hydrodynamic processes of heat and mass transfer under crystal growth and some results of parametric calculations for models of directional crystallization, fluid epitaxy and Chochralski method are presented in Polezhaev (1994).

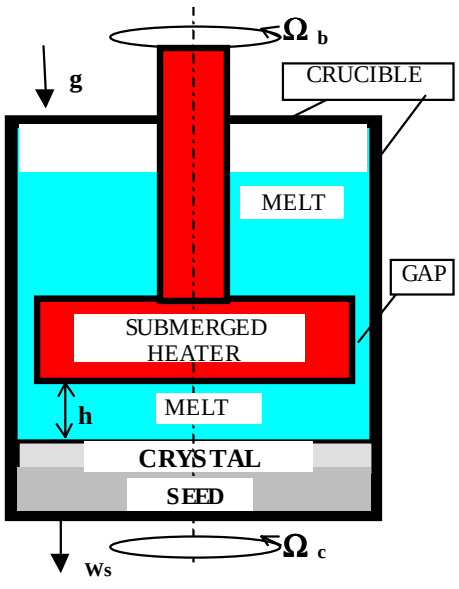

Fig.1 Scheme of the SHM method

This paper is devoted to numerical investigation of influence of monocrystal growth conditions on axial and radial distribution of dopant under crystallization of Ge doped Ga in a frame of Submerged Heater Method (SHM) crystal growth Fig.1, which is a vertical unidirectional method of crystallization with and without rotation and accurately controlled thermal conditions near crystallization surface. An interest to the method, which provides both thermal and geometrical ways of governing in accordance with classification Polezhaev (1994) is caused by two reasons: from one hand it allows accurately controlled thermal conditions of growth, which makes it promising for study kinetics and mechanisms of crystal growth, from other hand it allows to production of monocrystals under decreased natural convection, providing crystal growth conditions in terrestrial environment which are very close to space microgravity conditions. Primarily investigations on experimental and numerical analysis of dopant distribution in semiconductor monocrystals under such conditions have been performed by A. G. Ostrogorsky at al. (1995, 1997) (you can find references on more earlier their works in this work). The authors used two modifications of crystal growth methods: submerged buffle method and submerged heater method. Their study is not sufficient for detection of a set of conditions, which are necessary to provide reproducible results on dopant transfer in slow flow of the melt between crystallization surface and the buffle. This can be made by means of further experimental and numerical parametric calculation studies of heat and mass transfer in SHM crystal growth. Given paper is devoted to the numerical study SHM crystal growth with and without rotation of crucible and heater.

Numerical modeling has been provided in a frame of 2D unsteady Navier-Stokes equations and heat and mass transfer equations in cylindrical region. Utilization of unsteady formulation allowed detecting dopant distribution in growing crystal. Initial boundary value problem has been solved by the finite element method using hydrocode ASTRA conditions, geometry, rotation, gravity and growth rate on radial and axial distribution of the dopant has been investigated. The existence of optimal rates of

rotation to provide a homogeneous distribution of dopant is shown.

FORMULATION OF PROBLEM

Computational region is shown in Fig. 2, where 1 –

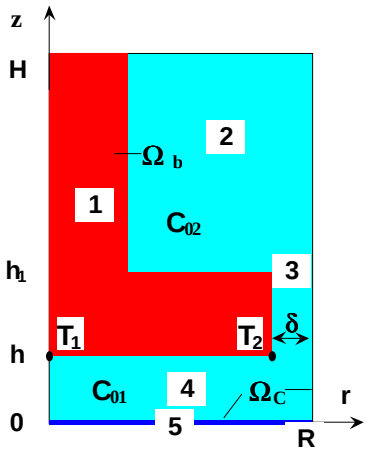

Fig.2. Computational region

heater, 2 - melt zone, 3 – gap, 4 – work melt zone, 5 - surface of crystal, R - radius of crucible, δ - size of gap, h - height of work zone, 0z - axis of symmetry.
The following assumptions have been in use: axial symmetry of the crystal growth process, height h of work zone 4, growth rate and thermal boundary conditions are permanent in time.

The Navier-Stokes-Boussinesq equations read:

$$\frac{\partial u}{\partial r}+\alpha\frac{u}{r}+\frac{\partial w}{\partial z}=0$$

$$\frac{du}{dt}-\alpha\frac{v^2}{r}=-\frac{1}{\rho_0}\frac{\partial p}{\partial r}+\frac{1}{r^\alpha}\frac{\partial}{\partial r}\left(r^\alpha\nu\frac{\partial u}{\partial r}\right)+\frac{\partial}{\partial z}\left(\nu\frac{\partial u}{\partial z}\right)-\alpha\nu\frac{u}{r^2}$$

$$\frac{dw}{dt}=-\frac{1}{\rho_0}\frac{\partial p}{\partial z}+\frac{1}{r^\alpha}\frac{\partial}{\partial r}\left(r^\alpha\nu\frac{\partial w}{\partial r}\right)+\frac{\partial}{\partial z}\left(\nu\frac{\partial w}{\partial z}\right)+g\beta(T-T_0)$$

$$\frac{dv}{dt}+\alpha\frac{uv}{r}=\alpha\left[\frac{1}{r}\frac{\partial}{\partial r}\left(r\nu\frac{\partial u}{\partial r}\right)+\frac{\partial}{\partial z}\left(\nu\frac{\partial u}{\partial z}\right)-\nu\frac{u}{r^2}\right]$$

$$\frac{d\rho c_p T}{dt}=\frac{1}{r^\alpha}\frac{\partial}{\partial r}\left(r^\alpha\lambda\frac{\partial T}{\partial r}\right)+\frac{\partial}{\partial z}\left(\lambda\frac{\partial T}{\partial z}\right)$$

$$\frac{dC}{dt}=\frac{1}{r^\alpha}\frac{\partial}{\partial r}\left(r^\alpha D\frac{\partial C}{\partial r}\right)+\frac{\partial}{\partial z}\left(D\frac{\partial w}{\partial z}\right)$$

where: u and w are velocities in r and z directions, v is the azimutal velocity, T is the temperature, C is dopant concentration, p is the pressure, g is gravity acceleration, β_T is thermal expansion factor, ν is the viscosity factor, D is diffusion factors, α is the geometry factor, which equals to 0 for flat geometry or 1 for axial symmetry.
The boundary conditions read:
at the axis of symmetry

$$r=0\ ,\ u=0\ ,\ \frac{\partial w}{\partial r}=0\ ,\ v=0\ ,\ \frac{\partial T}{\partial r}=0\ ,\ \frac{\partial C}{\partial r}=0\ ;$$

at the surface of the crystal

$$z=0\ ,\ u=0\ ,\ w=-W_S\ ,\ v=2\pi r\Omega_C\ ,\ T=T_m\ ,$$

$$D\frac{\partial C}{\partial z}=W_S C(1-k_0);$$

on the wall of the crucible

$$r=R\ ,\ u=0\ ,\ w=0\ ,\ v=2\pi R\Omega_C\ ,$$

$$\frac{\partial T}{\partial r}=0\ \ (0<z<h)\ ,\ T=T_h\ \ (h<z<H)\ ,\ \frac{\partial C}{\partial r}=0\ ;$$

at the surface of the submerged heater

$$u=0\ ,\ w=0\ ,\ v=2\pi r\Omega_b\ ,\ \frac{\partial C}{\partial n}=0\ ,\ \frac{\partial T}{\partial n}=0$$ (on bottom heater $T=T_b(r)$, where $T_b(r)$ is linear function between value T_1 and T_2);

upper inlet boundary

$$z=H\ ,\ u=0\ ,\ \frac{\partial w}{\partial z}=0\ ,\ v=0\ ,\ T=T_h\ ,\ C=C_0\ .$$

Formulation of boundary conditions has principal meaning for correctness of the model and comparison with experimental data. In particular boundary conditions can vary in time.
Initial conditions read:

$$t=0\ ,\ u=0\ ,\ w=0\ ,\ v=0\ ,\ T=T_m\ ,$$

$$C=C_{01}(0\le z\le h_1),\ \ C=C_{02}(h_1<z<H).$$

The problem characterized by following parameters of similarity: Prandtl number $Pr=\nu\rho c_p/\lambda$, Reynolds numbers $Re_\Omega=\Omega_C R^2/\nu$, $Re=W_S R/\nu$, Grashof number $Gr=g\beta\Delta TR^3/\nu^2$, (or Rayleigh number Ra=GrPr) and Schmidt number $Sc=\nu/D$. In most cases the parameters had values: $Pr=0.01$, Re_Ω and $Re<10^3$, $Gr=0-10^6$, $Sc=10$.
The distribution of dopant in the crystal C_{cr} has been detected by history of concentration in the melt on the surface of crystallization C using following formula: $C_{cr}=k_0 C$, where: k_0 is *segregation* factor.

4. Numerical method

Briefly most essential features of used numerical method can be described in a following way. For a typical convection-diffusion equation

$$\frac{\partial \mathbf{A}}{\partial t}+\mathbf{u}\cdot\nabla\mathbf{A}=k\nabla^2\mathbf{A}+\mathbf{F}$$

the following variational implicit Bubnov-Galerkin self-conjugated finite difference scheme in time is used:

$$\int_V\left(\frac{A^{n+1}-A^n}{\Delta t^n}+\mathbf{u}^n\cdot\nabla A^{n+1}\right)\left(\delta A+\Delta t^n\mathbf{u}^n\cdot\nabla\delta A\right)d\mathbf{V}=$$

$$= \int_v \left(k_1 \nabla A^{n+1} \cdot \nabla \delta A + F^{n+1} \delta A\right) dV + \int_s k\mathbf{n} \cdot \nabla A^{n+1} \delta A dS$$

Here an exponential viscosity correction a la Samarski is used to provide monotonous behavior of solution:

$$k_1 = k\left(1 + \frac{0.5\max(Uh, U^2\Delta t)}{k}\right) + 0.5\max(Uh, U^2\Delta t)$$

Linear finite elements in space were used. Auxiliary algebraic problems were solved by non-matrix conjugate gradients method with preconditioning by diagonal approximation of stiffness matrix. Algorithm is unconditionally stable but for good accuracy time step should not differ much from the value of Courant's time step: $0.1\Delta t_C < \Delta t^n < 10\Delta t_C$, $\Delta t_C = \min(h_i / U_i^n)$. Incompressibility was handled by penalty method (first method), by pressure correction Poisson equationconju (second method), by use of vorticity-stream function formulation (third method) and by Chorin's artificial compressibility (forth method). Results are in a good accordance for all four used techniques. The algorithms are incorporated into known hydrocode "ASTRA" for 2D and 3D geometry.

5. Test results

Following test problems have been solved:
1)thermal convection in rectangular region with T=0 at left wall and T=1 at right wall and insulation horizontal walls, (international test problem published in Davis et al. (1983));
2) Wheeler's international test for Czochralski swirl flow Wheeler (1990);
3)stationary SHM problem of Ostrogorsky et al. (1995)
Results for problem 1 calculated by code ASTRA and independently by code COMGA are presented in Fig. 3 and Table 1.

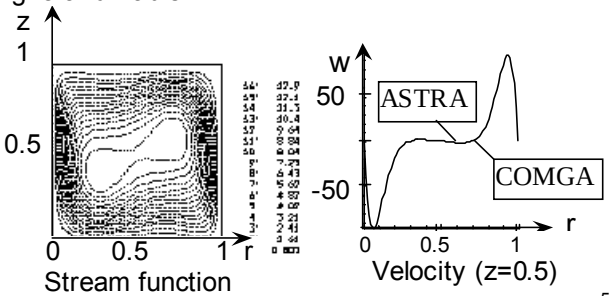

Fig. 3 Thermal convection in square cavity ($Ra=10^5$, $Pr=0.71$)

Table 1. Test convection problem ($Ra=10^5$, $Pr=0.71$).

Computer code	max ψ	Max v_x, x=0.5	max v_y y=0.5
"ASTRA"	13.703	49.958	96.421
"COMGA"	13.479	48.300	94.950
Benchmark	13.538	49.592	95.894

In table 1 maximum values of stream function, horizontal and vertical velocities calculated for test problem 1 using different computer codes are shown: "ASTRA" is the finite element code Bourago (1994) using grid 60x60, "COMGA" is the finite difference code using grid 65x65 (Ermakov et.al. (1992)), third row is benchmark solution, calculated in Davis et al. (1983) by extrapolation of set of finite difference solutions for different grids to the grid with "zero size of cell". Comparison shows that maximum difference between results of ASTRA and benchmark solution is not greater then 1.2%, while difference for "COMGA" is not greater then 2.5%. In Fig. 3 isolines of stream function and velocity profiles calculated using of ASTRA and COMGA codes almost consist.
Results of ASTRA were compared with numerical solution test problem 2 and 3. The comparison of results of given accounts with these test results has shown good concurrence. (for example, for problem 3 see Bourago et.al. 1997)

6. Influence of the value initial concentration on impurity distribution in crystal

The goal this path of the parametric calculations was to find conditions under which longitudinal distribution of dopant in the crystal becomes permanent while radial dopant distribution stays so homogeneous as possible.
Parametric calculations have been performed using code ASTRA for the following input data: $R = 0.016\,m$; $h = 0.008\ m$; $h_1 = 0.016\ m$; $H = 0.032\ m$; $\delta = 10^{-3} m$; $T_m = 936C^o$; $T_h = 956^oC$; $T_1 = 942^oC$; $T_2 = 945^oC$. Table 2 contains: N is a number of variant; $W_s = 0.01 - 10\,cm/hour$ is growth rate; $n = C_{01}/C_{02}$ is the ratio of initial concentrations ($C_{01} = 1$ is the concentration under heater, C_{02} is the concentration above heater); sign dC/dt is calculated value of time derivative of dopant concentration for $t=t_{max}$; g/g_o - dimensionless gravity acceleration (g_o - terrestrial).
Distribution of Ga in Ge is demonstrated in Fig. 4. These are results of parametric calculations of variants from Table 2. Number of variant in Fig. 4 is indicated at the left. Hereinafter referring on this or that variant in Figure 4 we shall write "Fig.4.number of variant".
Table 2 Variants of calculations

N	g/go	W_s	n	sign dC/dt	t_{max}
		cm/h		(r=1, z=0, $t=t_{max}$)	hours
1	0	1	10	+	3,29
2	1	0,01	16.67	-	8,2
3	1	10	16.67	-	1,32
4	1	1	1.667	+	1,29
5	1	1	10	0	1,09
6	1	3,6	10	-	1,16

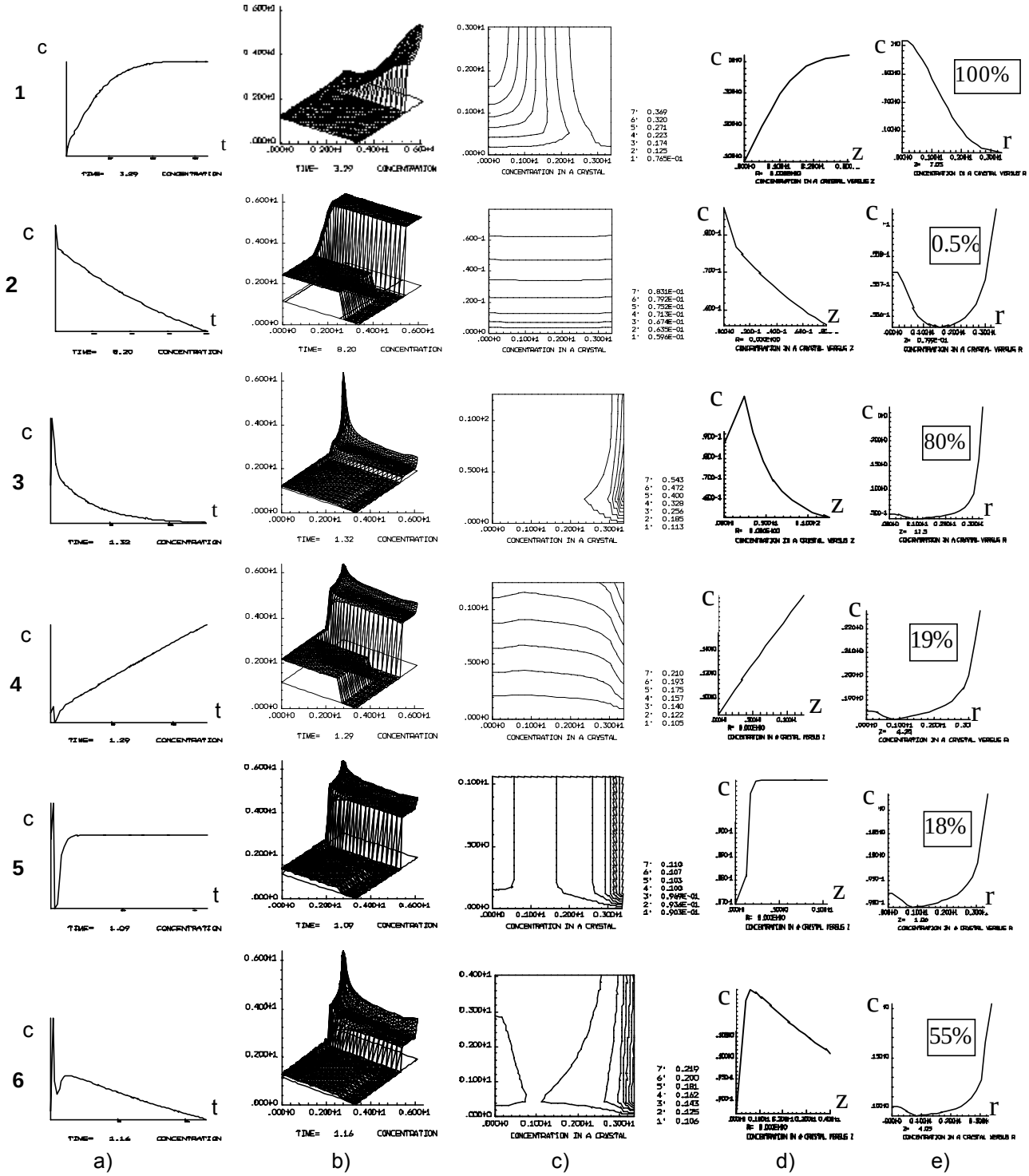

Fig. 4. Distribution of Ga in Ge. Results of parametric calculations of variants from Table 1 (numbers pointed on the left sides), a)- dopant concentration versus time for r=1 and z=0 b) concentration of dopant for t= t_{max}, c) contour lines of concentration in the crystal, d) distribution of dopant along vertical axis of crystal for r=0, e) radial distribution of dopant in the crystal for t= t_{max} (percentage of maximum in homogeneity is pointed).

In Fig.4 there are 5 pictures for each variant: a) concentration of dopant versus time for r=1 and z=0, b) concentration of dopant in the melt for $t=t_{max}$, c) contour lines of dopant concentration in the crystal, d) distribution of dopant along vertical axis of crystal for r=0, e) radial distribution of dopant in the crystal for $t=t_{max}$ (value of $(C_{max}-C_{min})/C_{max}\cdot 100\%$ is pointed).

The structure of convection flow becomes steady after several minutes; temperature gets steady after several seconds. However, the dopant concentration permanently varies during a whole process and does not reach stationary values. Only some quasi-stationary state after several hours is reached. The intensity of convection in work zone 4 is much less than in the region 2 above heater and can be practically excluded by special choice of radial temperature gradients. It should be pointed out that for all variants the melt flows in counter-clockwise direction. The direction of the flow can be changed if $T_1 > T_2$. The calculations have shown, that the control by thermal conditions (for example, when $T_b(r) = \text{const}$) allows for SHM on ground to receive conditions close to conditions of a microgravitation.

A case of absence of natural convection (Fig. 4#1) does not lead to homogeneous distribution of dopant because forced convection (a melt flow from region 2 through the gap δ into the region 4 due to crystal growth and relative motion of crucible and heater) violates homogeneity of dopant distribution near interface of crystal. Weak $(Ra < 10)$ natural convection (without forced convection) also violates homogeneity of dopant distribution because the dopant $(Sc = 10)$ is very sensitive to convection flows. Therefore there exist some optimal conditions of balance between natural and forced convection flows when they compensate each other and provide the almost homogeneous distribution of dopant.
These conditions depend on growth rate, size of the gap δ, thermal conditions and values of initial concentrations C_{01} and C_{02}. In calculations such conditions have been found: it is variant 5 (Fig. 4#5).

Results of parametric calculations, presented in Fig. 4, can be systematized as follows:

- The concentration is increasing in time (or along axis of crystal) $(dC/dt > 0)$ in variants 1, 4 (Fig.4#1a and Fig.4#4a), is almost permanent in variant 5 and is decreasing in all other variants $(dC/dt > 0)$.
- With increase of growth rate non-homogeneity increases - it is seen by comparison of variants 2 (Fig.4#2) with 3 (Fig.4#3) and 5 (Fig.4#5) with 6 (Fig.4#6).
- The dependence of non-homogeneity of dopant distribution on ratio initial values of concentration n is illustrated that with increase of n value of $|dC/dt|$ (or $|dC/dz|$ in the crystal) is decreasing.
- The influence of gravity acceleration can be observed by comparison of variants 1 ($g/g_0 = 0$) and 5 ($g/g_0 = 1$). In this case homogeneity is better if $g/g_0 = 1$.
- Radial non-homogeneity is minimal in variants 2 (Fig.4#2e), maximal in variant 1 (Fig.4#1e).
- Axial non-homogeneity is minimal in variant 5 (Fig.4#5d).

7. Results of calculations with rotation

To investigate an influence of rotation of the heater and the crucible on distribution of dopant in the crystal parametric calculations have been performed under following input data: $W_s = 1$ cm/hour, $C_{01} = C_{02} = 1$. All other parameters were the same as well as in paragraph 6 and values of frequencies indicated in Table 3. .
Table 3 contains: N is a number of run; $\Delta C = \max_r(C(r,z=0)) - \min_r(C(r,z=0))$ and t_{max} is maximal time of crystal growth process calculated .

Table 3. Script of runs.

N	g/g_0	Ω_b	Ω_c	f	ΔC	t_{max}
		rps	rps	Hz		Sec
1	1	0	0	0	0.198	3880
2	0	0	0	0	0.275	17100
3	1	0.05	0	0	0.263	5330
4	0	0.05	0	0	0.077	1940
5	1	0.3117	0	0	0.192	3650
6	0	0.3117	0	0	0.100	1030
7	1	0.6217	0	0	0.077	1410
8	1	0	0.3117	0	0.061	3640
9	1	0.05	0.3117	0	0.075	2310
10	1	-0.05	0.3117	0	0.049	3630
11	1	-0.3117	0.3117	0	0.054	2440
12	1	0.3117	0	0.68	0.279	1620

No gravity convection and no rotation (run 2). For $k_0 \neq 1$ while the following conditions are fulfilled:

$t < \frac{h}{W_s} \wedge C_{01} = C_{02} \wedge g = 0$ the distribution of dopant stays almost homogeneous on the interface melt-crystal and then for greater moments of time inhomogenuity can become essential. For $k_0 = 1$ and $C_{01} = C_{02}$ the dopant distribution stays homogeneous.

No rotation, convection is present (run 1). Natural convection leads to more homogeneous dopant distribution near interface of crystal. In Fig. 6a (run 1)

it is seen, that concentration of dopant is higher near wall of crucible then near axis of symmetry. This is qualitative difference of this case from the case of run 2 (without natural convection). This happens because a one-vortex flow of the melt in work zone 4 is directed in clockwise direction. Flow in upper region 2 has the same direction. Varying the thermal conditions on the wall of crucible or on the surface of submerged heater it is possible to get more homogeneous radial dopant distribution in the crystal and as well in particular it is possible to get the distribution of dopant which is very close to the one in case of microgravity g/g0=0 (run 2).

In Fig. 6 the distributions of dopant in the crystal were calculated for normal gravity on the Earth and for low gravity in space. No rotation was applied. Maximal values of dopant concentration are situated near axis of symmetry for microgravity space conditions and near wall of crucible in terrestrial environment when influence of thermo-gravitational convection becomes essential.

Influence of rotation.

In Fig.5 are shown stream functions without and with rotation of the heater ($\Omega_b = 0.3117$ rps).

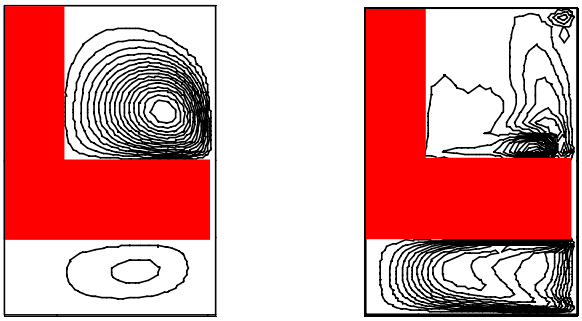

a) b)

Fig.5 Stream function on the Earth for SHM
a) without rotation (run 1), b) with rotation of the heater (run 5), see Table 3.

Rotation of heater lead to dopant distributions shown in Fig. 7 and 8. More fast rotation of heater (Fig. 8) provides more homogeneous distribution of dopant. Perhaps the rotation of crucible is more efficient as it can be seen from comparison of results for very fast rotating heater or crucible presented in Fig.9. The homogeneity can be improved if simultaneous rotation of heater and crucible is applied (Fig. 10). The best case if they are rotating in opposite directions. Heater should not be rotating too fast (Fig.10a) and there are no sense to apply oscillatory rotation (Fig.10b).

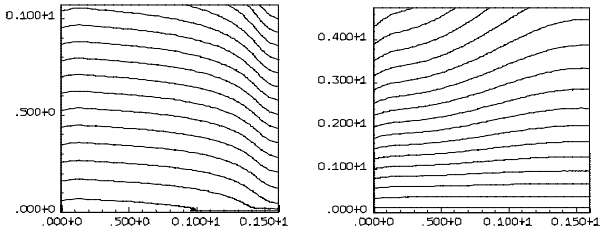

a) b)

Fig. 6. Modes of dopant distribution in the crystal without rotations.
a) On the Earth (run 1), b) In Space (run 2).

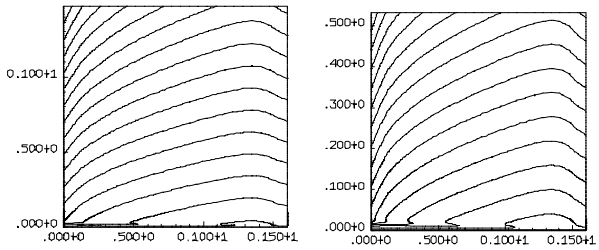

a) b)

Fig.7 Modes of dopant distribution in the crystal (runs 3,4).
a) On the Earth, rotating heater $\Omega_b = 0.05$ rps ;
b) In Space, rotating heater $\Omega_b = 0.05$ rps ;

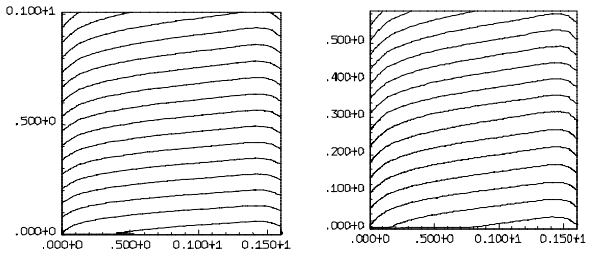

a) b)

Fig.8 Modes of dopant distribution in the crystal (runs 5-6).
a) On the Earth, rotating heater $\Omega_b = 0.3117$rps ;
b) In Space, rotating heater $\Omega_b = 0.3117$rps ;

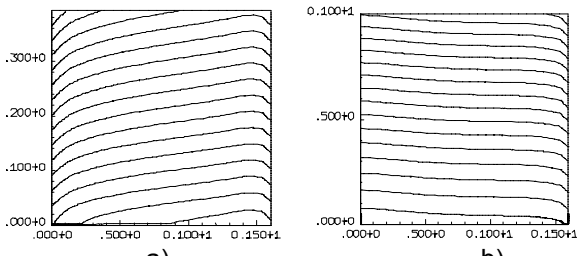

a) b)

Fig.9 Modes of dopant distribution in the crystal (runs 7-8).
a) On the Earth, rotating heater $\Omega_b = 0.6217$rps ;
b) On the Earth, rotating crucible $\Omega_C = 0.3117$rps ;

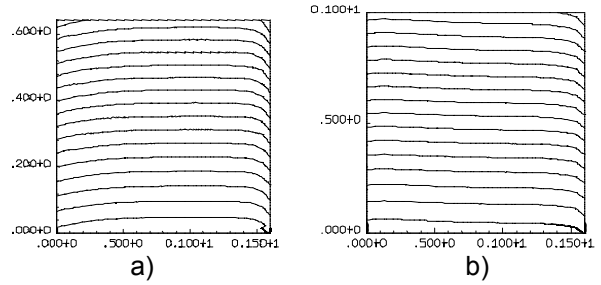

a) b)

Fig.10 Modes of dopant distribution in the crystal (runs 9-10).
a) On the Earth, rotating heater $\Omega_b = 0.05$ rps and crucible $\Omega_C = 0.3117$rps ;
b) On the Earth, rotating heater $\Omega_b = -0.05$ rps and crucible $\Omega_C = 0.3117$rps ;

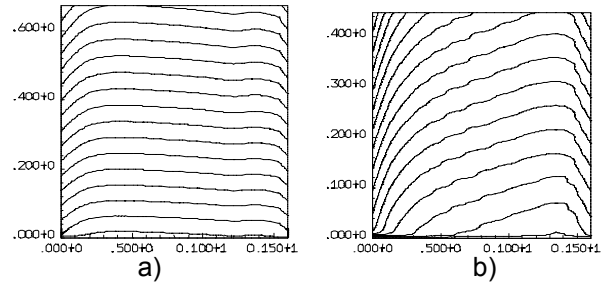

a) b)

Fig.11 Modes of dopant distribution in the crystal (runs 11-12).
a) On the Earth, rotating heater $\Omega_b = -0.3117$ rps and crucible $\Omega_C = 0.3117$rps ;
b) On the Earth, rotating heater $\Omega_b = 0.05$ rps and crucible $\Omega_C = 0$. Oscillatory rotation with f = 0.68 Hz.

Rotation causes an additional convection in opposite direction to the thermo-gravitational convection flow. Fight between these to flows lead to a better mixing of dopant and may level the dopant distribution on the interface of crystal. This fight takes place in both subregions above (subregion 2 in Fig.2) and below heater (subregion 4 in Fig.2). It accelerates vortex flow in subregion 2 and compensates natural convection in subregion 4 near interface of the crystal. Even in the case of steady rotation the flow slightly oscillates especially in subregion 2.
Well-known drawback of non-rotating mode of crystal growth in terrestrial environment is an existence of peak of concentration in the crystal near wall of crucible under the gap. The rotation can help in fight against this drawback. Our calculations indicate that most homogeneous radial distribution of dopant in the crystal may be provided by simultaneous opposite rotation of crucible and heater (run 10, Fig.10b). Calculations of oscillatory rotation of heater show that the distribution of dopant in the crystal is characterized also by similar oscillations of concentration (Fig.11b)

CONCLUSION

The modes of SHM crystal growth process which provide almost permanent longitudinal dopant distribution in Ge crystals dopant by Ga are found in numerical modeling (Fig. 4#5).
From results of calculations can make a conclusion that there is principal possibility to provide space conditions using SHM crystal growth method and special thermal conditions.
Rotation can lead to more homogeneous distribution of dopant in the crystal. Optimal rate of rotation depends on other physical, mechanical and geometrical conditions.
So the numerical modeling is necessary for detection of these optimal values in every particular case: changes in geometry, in rate of crystal growth, in temperature distribution, in gravity acceleration will lead to various values of optimal rates of rotation.

AKNOWLIDGEMENTS

The research was conducted on behalf of joint project TM-4 of Russian Space Agency and NASA.

NOMENCLATURE

c_p specific heat [J/kg/K]
f frequency of oscillatory rotation of the heater [Hz];
g gravitational acceleration [m s^{-2}];
g_0 terrestrial gravity acceleration [m s^{-2}];
h height of work zone [m];
k_0 segregation factor;
n normal
p pressure [N/m^2];
r radial coordinate [m];
t time coordinate;
u, v, w radial, circumferential and axial velocities [m/s];
z axial coordinate [m];
C dimensionless concentration of impurity in a melt;
C_{cr} dimensionless concentration of impurity in a crystal;
C_{01}, C_{02} initial dimensionless concentration;
ΔC difference of concentractions
D mass diffusion factor [m^2/s];
H height of computational region [m];
Gr Grashof number;
Pr Prandtl number;
R radius of the crucible;
Ra Rayleigh numbers;
Re Reynolds numbers;
Sc Schmidt numbers;
T temperature [K];
$T_b(r)$ temperature at the submerged heater [K];

T_h temperature on the top region [K];

T_m temperature of crystallization [K];

T_0 initial temperature [K];

W_s rate of crystal growth [m/s];

Greek symbols:

α geometry factor

δ size of a gap;

β_T coefficient of volumetric thermal expansion [K^{-1}];

λ thermal conductivity [W m^{-1} K^{-1}];

ν kinematic viscosity [m^2/s];

ρ_0 density [kg m^{-3}];

ψ stream function;

Ω_b frequency of rotation of the heater [rps];

Ω_C frequency of rotation of the crucible [rps];

REFERENCES

Bourago N.G., 1994, "Computer code "ASTRA" for nonlinear problems in continuum mechanics," *Abstracts of 7th Nordic Seminar on Computational Mechanics,* Trondheim, pp.101-102

Bourago N.G., 1997, V.D.Golyshev, M.A.Gonik, V.I.Polezhaev, A.I.Fedyushkin, V.B.Tsvetovski, Modes of forced and natural convection and their influence on dopant distribution in a crystal under crystal growth method OTF1a, *IIIth Int. Conf. "Crystals: Growth, Properties, Real Structure, Application", Alexandrov, Proc. of Conf.* vol.2, pp.116-131.

Bourago N.G., 1997, A.I.Fedyushkin, V.I.Polezhaev, "Modelling of unsteady submerged heating crystal growth in ground-based and microgravity environment," *Physical sciences in microgravity. Proceedings of joint Xth European and VI-th Russian Symposium on Physical sciences in microgravity. St. Petersburg, Russia, 15-21 June 1997,* Vol.II, pp.170-174.

Bourago N.G., 1998, A.I.Fedyushkin, V.I.Polezhaev, The influence of steady and oscillatory rotation on distribution of dopant in acrystal grown by submerged heating method. *Abstracts of 12th International conference on crystal growth (ICCCG-12), July 26-31, 1998, Jerusalem, Israel,* p.176

Bourago N.G., 1998, A.I.Fedyushkin, V.D.Golyshev, M.A.Gonik, V.I.Polezhaev, V.B.Tsvetovski, Experimental and mathematical study of dopant distribution in axial temperature flux method (ATF method). *Abstracts of 12th International conference on crystal growth (ICCCG-12), July 26-31, 1998, Jerusalem, Israel,* p.183

Davis de Vahl, 1983, I.P.Jones. Natural convection in square cavity: A comparison exercise. Intern. J. *Numer. Meth. Fluids.* Vol. 3, pp. 227-248.

Ermakov M.K., 1992, V.L.Griaznov, S.A.Nikitin et al. A PC-based System for Modelling Convection in Enclosures on the basis of Navier-Stokes Equations, Intern. *Journal Numer. Methods in Fluids*, v.15, pp.975-984.

Golyshev V.D., 1995, M.A.Gonik.Terrestrial experimental researh of new method features of large single crystal growth. In: *Proc. Microgravity sci. and aplications session, Int. Aerospace Congr., Moscow, August 16-17,1994*,Moscow, pp.167-171.

Meyer S., 1997, A.G.Ostrogorsky, "Forced convection in vertical Bridgman configuration with the submerged heater," *J.Crystal Growth* 171, 566-576.

Nikitin S.A., 1981, V.I.Poleshaev and A.I.Fedyushkin. Mathematical simulation in crystals prepared under microgravity conditions. *J.Crystal Growth*,52, pp.471-477.

Ostrogorsky A.G., 1995, and Z.Dragojlovic, *Proc. Microgravity sci. and applications session, Intern. Aerospace Congr., Moscow, August 16 - 17 , 1994* , Moscow , pp 127-133

Polezhaev V.I., 1991, et al. *Mathematical modeling of convective heat and mass transfer using Navier-Stokes equations.* Moscow, "Nauka".

Polezhaev V.I., 1994, Modeling of hydrodynamics, heat and mass transfer processes on the basis of unsteady Navier-Stokes equations. Applications to the material sciences at earth and under microgravity. *Comput. Methods Appl. Mech. Eng.* 115, 79-92

Wheeler A.A., 1990, Four test problems for the numerical simulation of flow in Czohralski crystal growth. *J.Crystal Growth* 102, 1990, 691-695.

Zharikov E.V., 1990, L.V.Prihod'ko, N.R.Storozhev. Fluid flow formation resulting from forced vibration of a growing crystal. *J.Crystal Growth,*99, pp.910-914.